7-16-2018

Neutrino Interferometry for High-Precision Tests of Lorentz Symmetry with IceCube

Karen Andeen
Marquette University, karen.andeen@marquette.edu

IceCube Collaboration

Accepted version. *Nature Physics*, Vol. 14 (2018):961-699. DOI.
A complete list of authors available in article text.

Nature Physics, Vol. 14, No. 9 (September 2018): 961-966. DOI.

Neutrino interferometry for high-precision tests of Lorentz symmetry with IceCube

Karen Andeen

Department of Physics, Marquette University, Milwaukee, WI

The IceCube Collaboration

(See complete list of IceCube contributors at end of article.)

Abstract

Lorentz symmetry is a fundamental spacetime symmetry underlying both the standard model of particle physics and general relativity. This symmetry guarantees that physical phenomena are observed to be the same by all inertial observers. However, unified theories, such as string theory, allow for violation of this symmetry by inducing new spacetime structure at the quantum gravity scale. Thus, the discovery of Lorentz symmetry violation could be the first hint of these theories in nature. Here we report the results of the most precise test of spacetime symmetry in the neutrino sector to date. We use high-energy atmospheric neutrinos observed at the IceCube Neutrino Observatory to search for anomalous neutrino oscillations as signals of Lorentz violation. We find no evidence for such phenomena. This allows us to constrain the size of the dimension-four operator in the standard-model extension for Lorentz violation to the 10^{-28} level and to set limits on higher-dimensional operators in this framework. These are among the most stringent limits on Lorentz violation set by any physical experiment.

Main

Very small violations of Lorentz symmetry, or Lorentz violation (LV), are allowed in many ultrahigh-energy theories, including string theory[1], non-commutative field theory[2] and supersymmetry[3]. The discovery of LV could be the first indication of such new physics. Worldwide efforts are therefore underway to search for evidence of LV. The standard-model extension (SME) is an effective-field-theory framework to systematically study LV[4]. The SME includes all possible types of LV that respect other symmetries of the standard model such as energy–momentum conservation and coordinate independence. Thus, the SME can provide a framework to compare results of LV searches from many different fields such as photons[5,6,7,8], nucleons[9,10,11], charged leptons[12,13,14] and gravity[15]. Recently, neutrino experiments have performed searches for LV[16,17,18]. So far, all searches have obtained null results. The full list of existing limits from all sectors and a brief overview of the field are available elsewhere[19,20]. Our focus here is to present the most precise test of LV in the neutrino sector.

The fact that neutrinos have mass has been established by a series of experiments[21,22,23,24,25,26]. The field has incorporated these results into the neutrino standard model (*ν*SM)—the standard model with three massive neutrinos. Although the *ν*SM parameters are not yet fully determined[27], the model is rigorous enough to be brought to bear on the question of LV. In the Methods, we briefly review the history of neutrino oscillation physics and tests of LV with neutrinos.

To date, neutrino masses have proved to be too small to be measured kinematically, but the mass differences are known via neutrino oscillations. This phenomenon arises from the fact that production and detection of neutrinos involves the flavour states, while the propagation is given by the Hamiltonian eigenstates. Thus, a neutrino with flavour $|\nu_\alpha\rangle$ can be written as a superposition of Hamiltonian eigenstates $|\nu_i\rangle$; that is, $|\nu_\alpha\rangle = \sum_{i=1}^{3} V_{\alpha i}(E)|\nu_i\rangle$,where V is the unitary matrix that diagonalizes the Hamiltonian and, in general, is a function of neutrino energy E. When the neutrino travels in vacuum without new physics, the Hamiltonian depends only on the neutrino masses, and the Hamiltonian eigenstates coincide with the mass eigenstates. That is, $H = \frac{1}{2E} U^\dagger \mathrm{diag}(m_1^2, m_2^2, m_3^2) U$, where m_i are the neutrino masses and U is the Pontecorvo–Maki–Nakagawa–Sakata matrix that diagonalizes the mass matrix m (ref. [27]).

A consequence of the flavour misalignment is that a neutrino beam that is produced purely of one flavour will evolve to produce other flavours. Experiments measure the number of neutrinos of different flavours, observed as a function of the reconstructed energy of the neutrino, E, and the distance the beam has travelled, L. The microscopic neutrino masses are directly tied to the macroscopic neutrino oscillation length. In this sense, neutrino oscillations are similar to photon interference experiments in their ability to probe very small scales in nature.

Lorentz-violating neutrino oscillations

Here, we use neutrino oscillations as a natural interferometer with a size equal to the diameter of Earth. We look for anomalous flavour-changing effects caused by LV that would modify the observed energy and zenith angle distributions of atmospheric muon neutrinos observed in the IceCube Neutrino Observatory[28] (see Fig. 1). Beyond flavour change due to small neutrino masses, any hypothetical LV fields could contribute to muon neutrino flavour conversion. We therefore look for distortion of the expected muon neutrino distribution. As this analysis does not distinguish between a muon neutrino (ν_μ) and its antineutrino ($\overline{\nu}_\mu$), when the word 'neutrino' is used, we are referring to both.

Fig. 1: Test of LV with atmospheric neutrinos.

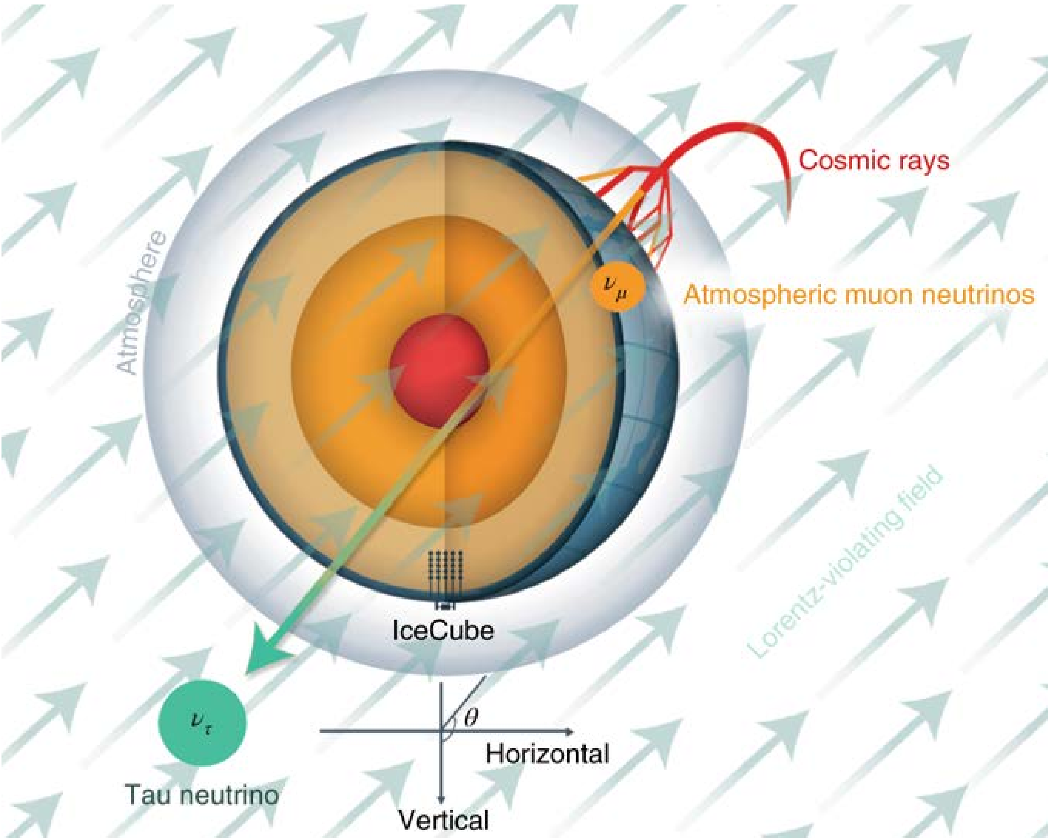

Muon neutrinos are produced in the upper atmosphere by the collisions of cosmic rays with air molecules. These atmospheric muon neutrinos pass through the entire Earth and are then detected by IceCube in Antarctica. The LV, indicated by arrows, permeates space and could induce an anomalous neutrino oscillation to tau neutrinos. Therefore, a potential signal of LV is the anomalous disappearance of muon neutrinos. Note, here we test only the isotropic component.

Past searches for LV have mainly focused on the directional effect in the Sun-centred celestial-equatorial frame[19] by looking only at the time dependence of physics observables as direction-dependent physics appears as a function of Earth's rotation. However, in our case, we assume no time dependence, and instead look at the energy distribution distortions caused by direction- and time-independent isotropic LV. Isotropic LV may be a factor ~10^3 larger than direction-dependent LV in the Sun-centred celestial-equatorial frame if we assume that the new physics is isotropic in the cosmic microwave background frame[20]. It would be most optimal to simultaneously look for both effects, but our limited statistics do not allow for this.

To calculate the effect, we start from an effective Hamiltonian derived from the SME[4], which can be written as

$$H \approx \frac{m^2}{2E} + \mathring{a}^{(3)} - E\mathring{c}^{(4)} + E^2\mathring{a}^{(5)} - E^3\mathring{c}^{(6)} \cdots \quad (1)$$

The first term of equation (1) is from the νSM; however, its impact decreases at high energy. The remaining terms ($\mathring{a}^{(3)}$, $\mathring{c}^{(4)}$, $\mathring{a}^{(5)}$ and so on) arise from the SME and describe isotropic Lorentz-violating effects. The circle symbol on the top indicates isotropic coefficients, and the number in the bracket is the dimension of the operator. These terms are typically classified by charge, parity and time reversal (CPT) symmetry; CPT-odd ($\mathring{a}^{(d)}$) and CPT-even ($\mathring{c}^{(d)}$). Focusing on muon neutrino to tau neutrino ($\nu_\mu \rightarrow \nu_\tau$) oscillations, all SME terms in equation (1) can be expressed as 2 × 2 matrices, such as

$$\mathring{c}^{(6)} = \begin{pmatrix} \mathring{c}^{(6)}_{\mu\mu} & \mathring{c}^{(6)}_{\mu\tau} \\ \mathring{c}^{(6)*}_{\mu\tau} & -\mathring{c}^{(6)}_{\mu\mu} \end{pmatrix} \quad (2)$$

Without loss of generality, we can define the matrices so that they are traceless, leaving three independent parameters, in this case: $\mathring{c}^{(6)}_{\mu\mu}$, $\mathrm{Re}(\mathring{c}^{(6)}_{\mu\tau})$ and $\mathrm{Im}(\mathring{c}^{(6)}_{\mu\tau})$. The off-diagonal Lorentz-violating term $\mathring{c}^{(6)}_{\mu\tau}$ dominates neutrino oscillations at high energy, which is the main interest of this paper. In this formalism, LV can be described by an infinite series, but higher-order terms are expected to be suppressed. Therefore, most terrestrial experiments focus on searching for effects of dimension-three and -four operators; $\mathring{a}^{(3)}$ and $E\ \mathring{c}^{(4)}$ respectively. However, our analysis extends to dimension-eight; that is, $E^2\ \mathring{a}^{(5)}$, $E^3\ \mathring{c}^{(6)}$, $E^4\ \mathring{a}^{(7)}$and $E^5\ \mathring{c}^{(8)}$. Such higher orders are accessible by IceCube, which observes high-energy neutrinos where we expect an enhancement from the terms with dimension greater than four. In fact, some theories, such as non-commutative field theory[2] and supersymmetry[3], allow for LV to appear in higher-order operators. As an example, we expect dimension-six new physics operators of order $\frac{1}{M_{\mathrm{P}}^2} \approx 10^{-38}\mathrm{GeV}^{-2}$, where M_{P} is the Planck mass, which is the natural energy scale of the unification of all matter and forces including gravity. We assume that only one dimension is important at any given energy scale, because the strength of LV is expected to be different at different orders.

We use the $\nu_\mu \rightarrow \nu_\tau$ two-flavour oscillation scheme following ref. [29]. This is appropriate because we assume there is no significant interference with ν_e. Details of the model used in this analysis are given in the Methods. The oscillation probability is given by

$$P(\nu_\mu \rightarrow \nu_\tau) = -4V_{\mu 1}V_{\mu 2}V_{\tau 1}V_{\tau 2}\sin^2\left(\frac{\lambda_2 - \lambda_1}{2}L\right) \quad (3)$$

where $V_{\alpha i}$ are the mixing matrix elements of the effective Hamiltonian (equation (1)), and λ_i are its eigenvalues. Both mixing matrix elements and eigenvalues are a function of energy, νSM oscillation parameters and SME coefficients.

The IceCube neutrino observatory

The IceCube Neutrino Observatory is located at the geographic South Pole[30,31]. The detector volume is one cubic kilometre of clear Antarctic ice. Atmospheric muon neutrinos interacting on surrounding ice or bedrock may produce high-energy muons, which emit photons that are subsequently detected by digital optical modules (DOMs) embedded in the ice. The DOMs consist of a 25-cm-diameter Hamamatsu photomultiplier tube, with readout electronics, contained within a 36.5 cm glass pressure housing. These are installed in holes in the ice with roughly 125 m separation. There are 86 holes in the ice with a total of 5,160 DOMs, which are distributed at depths of 1,450 m to 2,450 m below the surface, instrumenting 1 Gt of ice. The full detector description can be found in an earlier study[31].

This detector observes Cherenkov light from muons produced in charged-current ν_μ interactions. Photons detected by the DOMs allow for the reconstruction of the muon energy and direction, which is related to the energy of the primary ν_μ. As the muons are above critical energy, their energy can be determined by measuring the stochastic losses that produce Cherenkov light. See earlier work28 for details on the muon energy proxy used in this analysis. In the teraelectronvolt (TeV) energy range, these muons traverse distances of the order of kilometres, and have a small scattering angle due to the large Lorentz boost, resulting in 0.75° resolution on the reconstructed direction at 1 TeV (ref. [32]). We use up-going muon data of TeV-scale energy from two years of detector operation[28] representing 34,975 events with a 0.1% atmospheric muon contamination.

Analysis set-up

To obtain the prediction for LV effects, we multiply the oscillation probability, given in equation (3), with the predicted atmospheric neutrino flux calculated using the matrix cascade equation (MCEq)[33]. These 'atmospheric neutrinos' originate from the decay of muons and various mesons produced by collisions of primary cosmic rays and air molecules, and consist of both neutrinos and antineutrinos. The atmospheric neutrinos have two main components: 'conventional', from pion and kaon decay, and 'prompt', from charmed meson decay. The conventional flux dominates at energies less than 18 TeV because of the larger production cross-section, whereas the harder prompt spectrum becomes relevant at higher energy. In the energy range of interest, the astrophysical neutrino contribution is small. We include it modelled as a power law with normalization and spectral index, ~ $\Phi E^{-\gamma}$. The absorption of each flux component propagating through Earth to IceCube is properly modelled[34,35]. Muon production from ν_μ charged-current events at IceCube proceeds through deep inelastic neutrino interactions as calculated in ref. [36].

The short distance of travel for horizontal neutrinos leads to negligible spectral distortion due to LV, whereas the long path length for vertical neutrinos leads to modifications. Therefore, if we compare the zenith angle distribution (ϑ) of the expectation from simulations and ν_μ data from $\cos\vartheta = -1.0$ (vertical) to $\cos\vartheta = 0.0$ (horizontal) (see Fig. 1), then one can determine the allowed LV parameters. Figure 2 shows the ratio of transition probabilities of vertical events to horizontal events. The data transition probability is defined by the ratio of observed events to expected events, and the simulation transition probability is defined by the expected events in the presence of LV to the number of events in the absence of LV. In the absence of LV, this ratio equals 1. Here, as an example, we show several predictions from simulations with different dimension-six LV parameters $|\mathring{c}_{\mu\tau}^{(6)}|$. In general, higher-order terms are more important at higher energies. To assess the existence of LV, we perform a binned Poisson likelihood analysis by binning the data in zenith angle and energy. We use 10 linearly spaced bins in cosine of zenith angle from −1.0 to 0.0 and 17 logarithmically spaced bins in reconstructed muon energy ranging from 400 GeV to 18 TeV. Systematic uncertainties are incorporated as nuisance parameters in our likelihood. We introduce six systematic parameters related to the neutrino flux prediction: normalizations of conventional (40% error), prompt (no constraint) and astrophysical (no constraint) neutrino flux components; ratio of pion and kaon contributions for conventional flux (10% error); spectral index of primary cosmic rays (2% error); and astrophysical neutrino spectral index (25% error). The absolute photon detection efficiency has been shown to have negligible impact on the exclusion contours in a search for sterile neutrinos that uses an equivalent analysis technique for a subset of the IceCube data considered here[34,37]. The impact of light propagation model uncertainties on the horizontal to vertical ratio is less than 5% at a few TeV, where this analysis is most sensitive[35]. Thus, the impact of these uncertainties on the exclusion contours is negligible.

Fig. 2: The ratio of vertical to horizontal neutrino transition probabilities at IceCube.

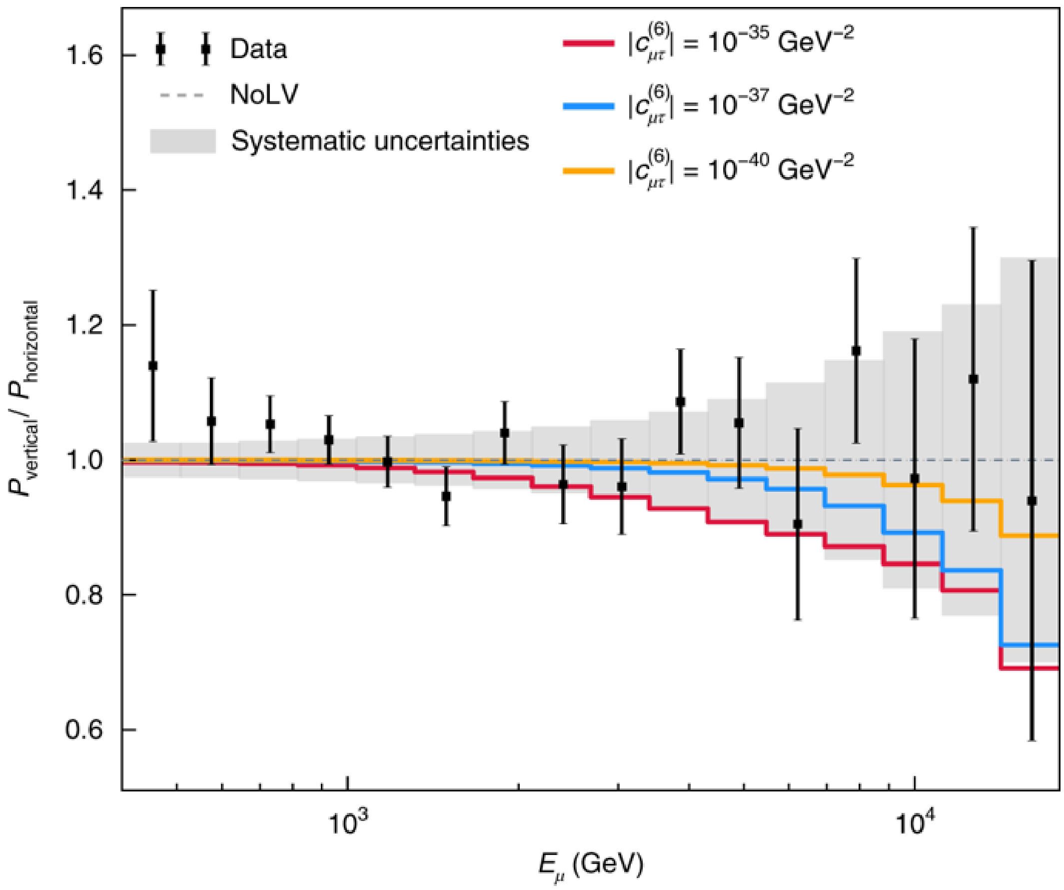

Here, vertical events are defined by cos$\vartheta \leq -0.6$ and the horizontal events are defined by cos$\vartheta > -0.6$. The transition probability ratio with 1 s.d. statistical errors (error bars), extracted from the data, is compared to the prediction for various dimension-six operator values. The range of uncorrelated systematic uncertainties is shown as a light grey band. This is constructed from ensembles of many simulations where the nuisance parameters are varied within their uncertainties.

To constrain the LV parameters, we use two statistical techniques. First, we performed a likelihood analysis by profiling the likelihood over the nuisance parameters per set of LV parameters. From the profiled likelihood, we find the best-fit LV parameters and derive the 90% and 99% confidence levels (CLs) assuming Wilks's theorem with three degrees of freedom[37]. Second, we set the priors to the nuisance parameter uncertainties and scan the posterior space of the likelihood by means of a Markov chain Monte Carlo (MCMC) method[38]. These two procedures are found to be complementary, and the extracted LV parameters agree with the null hypothesis. For simplicity, we present the likelihood results in this paper and show the MCMC results in the Methods.

Results

Figure 3 shows the excluded region of dimension-six SME coefficients. The results for all operators are available in the Supplementary Information. The fit was performed in a three-dimensional phase space; however, the complex phase of the off-diagonal terms is not important at high energy, and we choose the following representation methods. The horizontal axis shows the strength of LV, $\rho_6 \equiv \sqrt{(\mathring{c}^{(6)}_{\mu\mu})^2 + \mathrm{Re}(\mathring{c}^{(6)}_{\mu\tau})^2 + \mathrm{Im}(\mathring{c}^{(6)}_{\mu\tau})^2}$, and the vertical axis represents a fraction of the diagonal element, $\mathring{c}^{(6)}_{\mu\mu}/\rho_6$. The best-fit point shown by the marker is compatible with the absence of LV; therefore, we present 90% CL (red) and 99% CL (blue) exclusion regions. The contour extends to small values, beyond the phase space explored by previous analyses[16,17,18]. The leftmost edge of our exclusion region is limited by the small statistics of high-energy atmospheric neutrinos. The rightmost edge of the exclusion region is limited by fast LV-induced oscillations that suppress the flux but lead to no shape distortion. This can be constrained only by the absolute normalization of the flux. In the case of the dimension-three operator, the right edge can be excluded by other atmospheric neutrino oscillation measurements[18,39]. We have studied the applicability of Wilks's theorem via simulations. Near-degenerate real and imaginary parameters reduce the expected degrees of freedom from three and the results here are interpreted as conservative confidence intervals.

Fig. 3: The excluded parameter space region for the dimension-six SME coefficients.

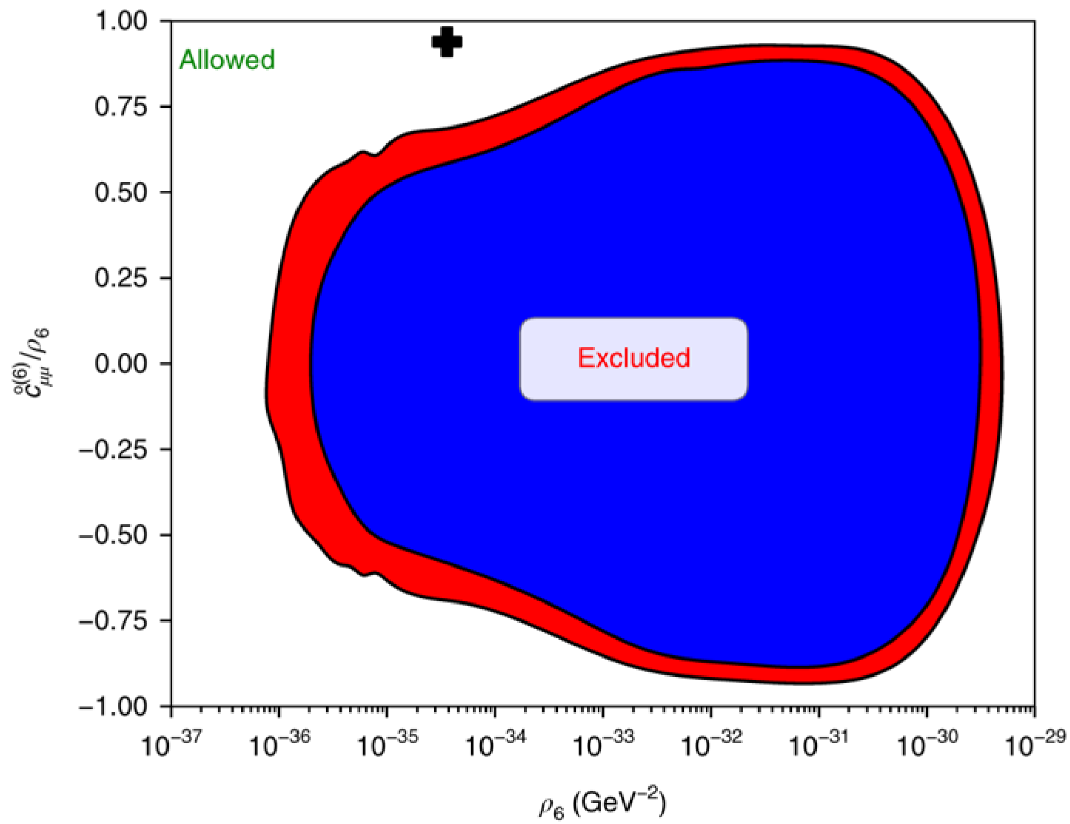

The figure shows the exclusion region of the dimension-six SME coefficients in the space of two parameters: ρ_6 and $\mathring{c}^{(6)}_{\mu\mu}/\rho_6$. Here, $\rho_6 \equiv \sqrt{(\mathring{c}^{(6)}_{\mu\mu})^2 + \mathrm{Re}(\mathring{c}^{(6)}_{\mu\tau})^2 + \mathrm{Im}(\mathring{c}^{(6)}_{\mu\tau})^2}$ (horizontal axis) and $\mathring{c}^{(6)}_{\mu\mu}/\rho_6$ (vertical axis) are a combination of the three SME coefficients: ρ represents LV strength, and $\mathring{c}^{(6)}_{\mu\mu}/\rho_6$ represents a fraction of the diagonal element, while the subscript 6 indicates the dimension. In the white region, LV is allowed. The best-fit point of this sample for this operator is shown by the black cross. The blue and red regions are excluded at 99% CL and 90% CL, respectively.

Unlike previous results[16,17,18], this analysis includes all parameter correlations, allowing for certain combinations of parameters to be unconstrained. This can be seen near $\mathring{c}^{(6)}_{\mu\mu}/\rho_6 = -1$ and 1, where LV is dominated by the large diagonal component. This induces the quantum Zeno effect[40], where a neutrino flavour state is 'arrested' in one state by a continuous interaction with a LV field suppressing flavour transitions. Thus, the unshaded regions below and above our exclusion zone are very difficult to constrain with terrestrial experiments.
Table 1 summarizes the results of this work along with representative best limits. A comprehensive list of LV tests is available in ref. [19]. To date, there is no experimental indication of LV, and all of these experiments have maximized their limits by assuming that all but one of the SME parameters are zero[19]. Therefore, to make our results comparable with previous limits, we adopt the same convention. For this, we set the diagonal SME

parameters to zero and focus on setting limits on the off-diagonal elements. The details of the procedure used to set limits are given in the Supplementary Information.

Table 1 Comparison of attainable best limits of SME coefficients in various fields

Dimension	Method	Type	Sector	Limits	Reference
Three	Cosmic microwave background polarization	Astrophysical	Photon	~10^{-43} GeV	5
	He-Xe co-magnetometer	Tabletop	Netron	~10^{-34} GeV	10
	Torsion pendulum	Tabletop	Electron	~10^{-31} GeV	12
	Muon g-2	Accelerator	Muon	~10^{-24} GeV	13
	Neutino oscillation	Atmospheric	Neutrino	$\left\|\mathrm{Re}\left(\mathring{a}^{(3)}_{\mu\tau}\right)\right\|, \left\|\mathrm{Im}\left(\mathring{a}^{(3)}_{\mu\tau}\right)\right\|$ $< 2.9 \times 10^{-24}\mathrm{GeV}(99\%\mathrm{CL})$ $< 2.0 \times 10^{-24}\mathrm{GeV}(90\%\mathrm{CL})$	This work
Four	Gamma-ray-burst (GRB) vacuum birefringence	Astrophysical	Photon	~10^{-38}	6
	Laser interferometer	Gravitational-wave observatory	Photon	~10^{-22}	7
	Sapphire cavity oscillator	Tabletop	Photon	~10^{-18}	8
	Ne-Rb-K co-magnetometer	Tabletop	Neutron	~10^{-29}	11
	Trapped Ca^+ ion	Tabletop	Electron	~10^{-19}	14
	Neutrino oscillation	Atmospheric	Neutrino	$\mathrm{Re}(\mathring{c}^{(4)}_{\mu\tau}), \|\mathrm{Im}(\mathring{c}^{(4)}_{\mu\tau})\|$ $< 3.9 \times 10^{-28}(99\%\mathrm{CL})$ $< 2.7 \times 10^{-28}(90\%\mathrm{CL})$	This work
Five	GRB vacuum birefringence	Astrophysical	Photon	~10^{-34} GeV^{-1}	6
	Ultrahigh-energy cosmic ray	Astrophysical	Proton	~10^{-22} to 10^{-18} GeV^{-1}	9
	Neutrino oscillation	Atmospheric	Neutrino	$\left\|\mathrm{Re}\left(\mathring{a}^{(5)}_{\mu\tau}\right)\right\|, \left\|\mathrm{Im}\left(\mathring{a}^{(5)}_{\mu\tau}\right)\right\|$ $< 2.3 \times 10^{-32}\mathrm{GeV}^{-1}(99\%\mathrm{CL})$ $< 1.5 \times 10^{-32}\mathrm{GeV}^{-1}(90\%\mathrm{CL})$	This work
Six	GRB vacuum birefringence	Astrophysical	Photon	~10^{-31} GeV^{-2}	6
	Ultrahigh-energy cosmic ray	Astrophysical	Proton	~10^{-42} to 10^{-35} GeV^{-2}	9
	Gravitational Cherenkov radiation	Astrophysical	Gravity	~10^{-31} GeV^{-2}	15
	Neutrino oscillation	Atmospheric	Neutrino	$\left\|\mathrm{Re}\left(\mathring{c}^{(6)}_{\mu\tau}\right)\right\|, \left\|\mathrm{Im}\left(\mathring{c}^{(6)}_{\mu\tau}\right)\right\|$ $< 1.5 \times 10^{-36}\mathrm{GeV}^{-2}(99\%\mathrm{CL})$ $< 9.1 \times 10^{-37}\mathrm{GeV}^{-2}(90\%\mathrm{CL})$	This work
Seven	GRB vacuum birefringence	Astrophysical	Photon	~10^{-28} GeV^{-3}	6
	Neutrino oscillation	Atmospheric	Neutrino	$\left\|\mathrm{Re}\left(\mathring{a}^{(7)}_{\mu\tau}\right)\right\|, \left\|\mathrm{Im}\left(\mathring{a}^{(7)}_{\mu\tau}\right)\right\|$ $< 8.3 \times 10^{-41}\mathrm{GeV}^{-3}(99\%\mathrm{CL})$ $< 3.6 \times 10^{-41}\mathrm{GeV}^{-3}(90\%\mathrm{CL})$	This work
Eight	Gravitational Cherenkov radiation	Astrophysical	Gravity	~10^{-46} GeV^{-4}	15
	Neutrino oscillation	Atmospheric	Neutrino	$\left\|\mathrm{Re}\left(\mathring{c}^{(8)}_{\mu\tau}\right)\right\|, \left\|\mathrm{Im}\left(\mathring{c}^{(8)}_{\mu\tau}\right)\right\|$ $< 5.2 \times 10^{-45}\mathrm{GeV}^{-4}(99\%\mathrm{CL})$ $< 1.4 \times 10^{-45}\mathrm{GeV}^{-4}(90\%\mathrm{CL})$	This work

Let us consider the limits from the lowest to highest order. Dimension-three and -four operators are included in the renormalizable sector of SME. These are the main focus of experiments using photons[7,8], nucleons[10,11] and charged leptons[12,13,14]. Going beyond terrestrial experiments, limits arising from astrophysical observations provide strong constraints[5,6]. Among the variety of limits coming from the neutrino sector, the attainable best limits are dominated by atmospheric neutrino oscillation analyses[16,17,18], where the longest propagation length and the highest energies enable us to use neutrino oscillations as the biggest interferometer on Earth. The results from our analysis surpass past ones due to the higher statistics of high-energy atmospheric neutrinos and our improved control of systematic uncertainties. Using a traditional metric, which assumes neutrinos to be massless, we can recast our result as an upper limit on any deviation of the speed of massless neutrinos from the speed of light due to LV. That is less than 10^{-28} at 99% CL. This is about an order-of-magnitude improvement over past analyses[16,17,18], and is of the same order as the deviation in speed that is expected due to the known neutrino mass at the energies relevant for this analysis.

Searches of dimension-five and higher LV operators are dominated by astrophysical observations[6,9,15]. Among them, ultrahigh-energy cosmic rays have the highest measured energy[41] and are used to set the strongest limits on dimension-six and higher operators[9]. However, these limits are sensitive to the composition of ultrahigh-energy cosmic rays, which is currently uncertain[20,42]. These limits assume that the cosmic rays at the highest energies are protons, but if they are in fact iron nuclei, then the ultrahigh-energy cosmic ray limits are significantly reduced. Our analysis sets the most stringent limits in an unambiguous way across all fields for the dimension-six operator. Such high-dimension operators are generic signatures of new physics[43]. For example, the dimension-five operator is an attractive possibility to produce neutrino masses, and dimension-six operators represent new physics interactions that can, for example, mediate proton decay. Although LV dimension-six operators, such as $\mathring{c}_{\mu\tau}^{(6)}$, are well motivated by certain theories including non-commutative field theory[2] and supersymmetry[3], they have so far not been probed with elementary particles due to the lack of available high-energy sources. Thus, our work pushes boundaries on new physics beyond the standard model and general relativity.

Conclusion

We have presented a test of LV with high-energy atmospheric muon neutrinos from IceCube. Correlations of the SME coefficients are fully taken into account, and systematic errors are controlled by the fit. Although we did not find evidence for LV, this analysis provides the best attainable limits on SME coefficients in the neutrino sector along with limits on the higher-order operators. Comparison with limits from other sectors reveals that this work provides among the best attainable limits on dimension-six coefficients across all fields: from tabletop experiments to cosmology. This is a remarkable point that demonstrates how powerful neutrino interferometry can be in the study of fundamental spacetime properties.

Further improvements on the search for LV in the neutrino sector using IceCube will be possible when the astrophysical neutrino sample is included[44]. Such analyses[45,46] will require a substantial improvement of detector and flux systematic uncertainty evaluations[47,48]. In the near future, water-based neutrino telescopes such as KM3NeT[49] and the ten-times-larger IceCube-Gen2[50] will be in a position to observe more astrophysical neutrinos. With the higher statistics and improved sensitivity, these experiments will have an enhanced potential for discovery of LV.

Methods

Neutrino oscillations and tests of LV

The field of neutrino oscillations has been developed through a series of measurements of solar[51,52,53,54,55], atmospheric[56,57,58], reactor[59,60,61,62] and accelerator neutrinos[57,63,64]. In the early days, the cause of neutrino oscillations was not precisely known, and LV was suggested as a possible source of neutrino flavour anomalies[65] and so tests of LV with high-energy astrophysical sources started to generate a lot of interest[66]. Subsequently, the L/Edependence of standard neutrino oscillations was measured[56]. As the neutrino mass term in the effective Hamiltonian has a $1/E$ energy dependence, it was a strong indication that a non-zero neutrino mass is in fact the cause of neutrino oscillations, not LV. Then, the focus of the community shifted to consider LV to be a second-order effect in neutrino oscillations, and so neutrino oscillation data have been used to look for small deviations due to LV from the standard neutrino mass oscillations.

One approach to look for LV is to use a model-independent effective field theory, such as the SME[67,68,69]. The SME is widely used in communities from low-energy tabletop experiments to high-energy particle physics and cosmology, to search for LV. This formalism incorporates various fundamental features of quantum field theories, such as energy–momentum conservation, observer Lorentz transformations and spin statistics; however, it includes violations of particle Lorentz transformations. A number of neutrino oscillation data sets have been analysed using this formalism, including LSND[70], MiniBooNE[71], MINOS[72,73,74,75], Double Chooz[76,77], SNO[78] and T2K[79], as well as the aforementioned IceCube-40 and Super-Kamiokande. These experiments can be classified into two groups. First, the presence of a direction-dependent field induces direction-dependent physics. In particular, neutrino beam lines are fixed and so such direction-dependent physics would show up as a time-dependence of neutrino oscillation data[70,71,72,73,74,75,76,78,79]. Second, a search of LV is possible even without assuming the presence of a spatial component (that is, no time-dependent physics), by utilizing distortions of the spectrum[77]. The results presented here are based on this second approach.

Neutrino oscillation formula

Here, we illustrate how to calculate the oscillation probability for the case with non-zero isotropic LVs, such as $\mathring{a}^{(d)}$ and $\mathring{c}^{(d)}$. The effective Hamiltonian relevant for oscillation is given by

$$H \approx \frac{m^2}{2E} + \sum_{d\geq 3} E^{d-3}(\mathring{a}^{(d)} - \mathring{c}^{(d)})$$

Note that $\mathring{a}^{(d)}$ are non-zero for d = odd, and $\mathring{c}^{(d)}$ are non-zero for d = even. We assume that either one of them is non-zero. We use the $\nu_\mu \rightarrow \nu_\tau$ two-flavour approximation that allows us to solve the time-dependent Schrödinger equation analytically to derive the neutrino oscillation formula with neutrino masses and LV. This choice is allowed because a large matter potential 'arrests' ν_e(quantum Zeno effect[40]) and prevent transitions from ν_μ. As the matter potential of ν_e is much bigger than that due to LV effects, the size of LV that we consider here hardly induces any $\nu_\mu \rightarrow \nu_e$ transition. Our choice of the two-flavour oscillation model does not diminish the strength of our constraints on parameters in the $\nu_\mu - \nu_\tau$ block matrix with respect to a full three-flavour calculation. Hence, the mass matrix m^2 can be diagonalized to $M^2 = \mathrm{diag}(m_2^2, m_3^2)$ by a mixing matrix U with mixing angle ϕ,

$$\begin{aligned} m^2 &= UM^2U^\dagger \\ &= \begin{pmatrix} \cos\phi & \sin\phi \\ -\sin\phi & \cos\phi \end{pmatrix} \begin{pmatrix} m_2^2 & 0 \\ 0 & m_3^2 \end{pmatrix} \begin{pmatrix} \cos\phi & -\sin\phi \\ \sin\phi & \cos\phi \end{pmatrix} \end{aligned}$$

By adding $E^{d-3}(\mathring{a}^{(d)} - \mathring{c}^{(d)})$, this 2×2 Hamiltonian can be diagonalized with two eigenvalues, λ_1 and λ_2. Here, we define $\lambda_2 > \lambda_1$. Then the oscillation formula is

$$P(\nu_\mu \rightarrow \nu_\tau) = \frac{|2A_2|^2}{(\lambda_2 - \lambda_1)^2} \sin^2\left(\frac{\lambda_2 - \lambda_1}{2} L\right)$$

where

$$\lambda_1 = \frac{1}{2}\left[(A_1 + A_3) - \sqrt{|A_1 - A_3|^2 + |2A_2|^2}\right]$$
$$\lambda_2 = \frac{1}{2}\left[(A_1 + A_3) + \sqrt{|A_1 - A_3|^2 + |2A_2|^2}\right]$$
$$A_1 = \frac{1}{2E}(m_2^2\cos^2\phi + m_3^2\sin^2\phi) + E^{d-3}\left(\mathring{a}_{\mu\mu}^{(d)} - \mathring{c}_{\mu\mu}^{(d)}\right)$$
$$A_2 = \frac{1}{2E}\cos\phi\sin\phi(m_2^2 - m_3^2) + E^{d-3}\left(\mathring{a}_{\mu\tau}^{(d)} - \mathring{c}_{\mu\tau}^{(d)}\right)$$
$$A_3 = \frac{1}{2E}(m_2^2\sin^2\phi + m_3^2\cos\phi) - E^{d-3}\left(\mathring{a}_{\mu\mu}^{(d)} - \mathring{c}_{\mu\mu}^{(d)}\right)$$

In the high-energy limit, the neutrino mass effect is negligible in comparison to Lorentz-violating effects,

$$P(\nu_\mu \to \nu_\tau) \sim \left(1 - \frac{\left[\mathring{a}_{\mu\mu}^{(d)} - \mathring{c}_{\mu\mu}^{(d)}\right]^2}{\rho_d^2}\right)\sin^2(L\rho_d E^{d-3})$$
$$= \frac{\left|\mathring{a}_{\mu\tau}^{(d)} - \mathring{c}_{\mu\tau}^{(d)}\right|^2}{\rho_d^2}\sin^2(L\rho_d E^{d-3})$$

Here we use $\rho_d \equiv \sqrt{(\mathring{a}_{\mu\mu}^{(d)})^2 + \mathrm{Re}(\mathring{a}_{\mu\tau}^{(d)})^2 + \mathrm{Im}(\mathring{a}_{\mu\tau}^{(d)})^2}$ or $\sqrt{(\mathring{c}_{\mu\mu}^{(d)})^2 + \mathrm{Re}(\mathring{c}_{\mu\tau}^{(d)})^2 + \mathrm{Im}(\mathring{c}_{\mu\tau}^{(d)})^2}$, which represents the strength of LV. Then, $\mathring{a}_{\mu\mu}^{(d)}/\rho_d$ and $\mathring{c}_{\mu\mu}^{(d)}/\rho_d$ become fractions of diagonal terms that are bounded between −1 and +1. The result suggests that there are no LV neutrino oscillations without off-diagonal terms and that the LV oscillations are symmetric between the real and imaginary parts of the off-diagonal SME parameters.

Bayesian framework

The main results of this paper are extracted using Wilks's theorem so as to be directly comparable with frequentist results reported by other neutrino experiments. For completeness, we have also performed a Bayesian analysis that uses a joint distribution over the nine systematic and LV parameters. This joint distribution is constructed from the same likelihood and prior distributions used in the frequentist analysis, except that we also added conservative constraints on all flux normalizations to avoid a strong prior range dependence. The Bayesian study is presented in two results (see Supplementary Fig. 1), which were both generated by the EMCEE MCMC software package[38]. First, we constructed the 99% exclusion credibility region from a sampling of the joint distribution, with two different treatments on nuisance parameters. Second, we extracted the result based on the Bayes factor of marginalizing the likelihood over nuisance parameters using the MultiNest algorithm[80]. These studies highlight the differences in results obtained using different treatments of nuisance parameters.

Data availability

The data that were used in this study are available in the IceCube Public Data Access 'Astrophysical muon neutrino flux in the northern sky with 2 years of IceCube data'[28](http://icecube.wisc.edu/science/data/).

Additional information

Publisher's note: Springer Nature remains neutral with regard to jurisdictional claims in published maps and institutional affiliations.

References

1.Kostelecký, V. A. & Samuel, S. Spontaneous breaking of Lorentz symmetry in string theory. *Phys. Rev. D* **39**, 683–685 (1989).

2.Carroll, S. M., Harvey, J. A., Kostelecký, V. A., Lane, C. D. & Okamoto, T. Noncommutative Field Theory and Lorentz Violation. *Phys. Rev. Lett.* **87**, 141601 (2001).

1. 3.Groot Nibbelink, S. & Pospelov, M. Lorentz violation in supersymmetric field theories. *Phys. Rev. Lett.* **94**, 081601 (2005).

4.Kostelecký, A. & Mewes, M. Neutrinos with Lorentz-violating operators of arbitrary dimension. *Phys. Rev. D* **85**, 096005 (2012).

5.Komatsu, E. et al. Five-year Wilkinson microwave anisotropy probe (WMAP) observations: cosmological interpretation. *Astrophys. J. Suppl.* **180**, 330–376 (2009).

2. 6.Kostelecký, V. A. & Mewes, M. Constraints on relativity violations from gamma-ray bursts. *Phys. Rev. Lett.* **110**, 201601 (2013).
3. 7.Kostelecký, V. A., Melissinos, A. C. & Mewes, M. Searching for photon-sector Lorentz violation using gravitational-wave detectors. *Phys. Lett. B* **761**, 1–7 (2016).
4. 8.Nagel, M. et al. Direct terrestrial test of Lorentz symmetry in electrodynamics to 10^{-18}. *Nat. Commun.* **6**, 8174 (2015).
5. 9.Maccione, L., Taylor, A. M., Mattingly, D. M. & Liberati, S. Planck-scale Lorentz violation constrained by ultra-high-energy cosmic rays. *J. Cosmol. Astropart. Phys.* **0904**, 022 (2009).
6. 10.Allmendinger, F. et al. New limit on Lorentz-invariance- and CPT-violating neutron spin interactions using a free-spin-precession ^{3}He-^{129}Xe comagnetometer. *Phys. Rev. Lett.* **112**, 110801 (2014).
7. 11.Smiciklas, M., Brown, J. M., Cheuk, L. W. & Romalis, M. V. A new test of local Lorentz invariance using ^{21}Ne-Rb-K comagnetometer. *Phys. Rev. Lett.* **107**, 171604 (2011).
8. 12.Heckel, B. R. et al. New CP-violation and preferred-frame tests with polarized electrons. *Phys. Rev. Lett.* **97**, 021603 (2006).
9. 13.Bennett, G. W. et al. Search for Lorentz and CPT violation effects in muon spin precession. *Phys. Rev. Lett.* **100**, 091602 (2008).

14.Pruttivarasin, T. et al. A Michelson–Morley test of Lorentz symmetry for electrons. *Nature* **517**, 592–595 (2015).

15.Kostelecký, V. A. & Tasson, J. D. Constraints on Lorentz violation from gravitational Čerenkov radiation. *Phys. Lett. B* **749**, 551–559 (2015).

16.Abbasi, R. et al. Determination of the atmospheric neutrino flux and searches for new physics with AMANDA-II. *Phys. Rev. D* **79**, 102005 (2009).

17. Abbasi, R. et al. Search for a Lorentz-violating sidereal signal with atmospheric neutrinos in IceCube. *Phys. Rev. D* **82**, 112003 (2010).

18. Abe, K. et al. Test of Lorentz invariance with atmospheric neutrinos. *Phys. Rev. D* **91**, 052003 (2015).

19. Kostelecký, V. A. & Russell, N. Data tables for Lorentz and CPT violation. *Rev. Mod. Phys.* **83**, 11–31 (2011).

20. Liberati, S. Tests of Lorentz invariance: a 2013 update. *Class. Quant. Grav.* **30**, 133001 (2013).

21. Fukuda, Y. et al. Evidence for oscillation of atmospheric neutrinos. *Phys. Rev. Lett.* **81**, 1562–1567 (1998).

22. Ahmad, Q. R. et al. Measurement of the rate of $\nu_e + d \rightarrow p + p + e^-$ interactions produced by ^8B solar neutrinos at the Sudbury Neutrino Observatory. *Phys. Rev. Lett.* **87**, 071301 (2001).

23. Ahn, M. H. et al. Indications of neutrino oscillation in a 250 km long baseline experiment. *Phys. Rev. Lett.* **90**, 041801 (2003).

24. Eguchi, K. et al. First results from KamLAND: Evidence for reactor anti-neutrino disappearance. *Phys. Rev. Lett.* **90**, 021802 (2003).

25. Abe, K. et al. Indication of electron neutrino appearance from an accelerator-produced off-axis muon neutrino beam. *Phys. Rev. Lett.* **107**, 041801 (2011).

26. An, F. P. et al. Observation of electron-antineutrino disappearance at Daya Bay. *Phys. Rev. Lett.* **108**, 171803 (2012).

27. Esteban, I., Gonzalez-Garcia, M. C., Maltoni, M., Martinez-Soler, I. & Schwetz, T. Updated fit to three neutrino mixing: exploring the accelerator-reactor complementarity. *J. High Energy Phys.* **1701**, 087 (2017).

28. Aartsen, M. G. et al. Evidence for astrophysical muon neutrinos from the northern sky with IceCube. *Phys. Rev. Lett.* **115**, 081102 (2015).

29. Gonzalez-Garcia, M. C., Halzen, F. & Maltoni, M. Physics reach of high-energy and high-statistics IceCube atmospheric neutrino data. *Phys. Rev. D* **71**, 093010 (2005).

30. Abbasi, R. et al. The IceCube data acquisition system: signal capture, digitization, and timestamping. *Nucl. Instrum. Meth. A* **601**, 294–316 (2009).

31. Aartsen, M. G. et al. The IceCube Neutrino Observatory: instrumentation and online systems. *J. Instrum.* **12**, P03012 (2017).

32. Weaver, C. N. *Evidence for Astrophysical Muon Neutrinos from the Northern Sky*. PhD thesis, Univ. Wisconsin–Madison (2015).

33. Fedynitch, A., Engel, R., Gaisser, T. K., Riehn, F. & Stanev, T. Calculation of conventional and prompt lepton fluxes at very high energy. *Eur. Phys. J. Web Conf.* **99**, 08001 (2015).

34. Jones, B. J. P. *Sterile Neutrinos in Cold Climates*. PhD thesis, MIT (2015).

35. Argüelles Delgado, C. A. *New Physics with Atmospheric Neutrinos*. PhD thesis, Univ. Wisconsin–Madison (2015).

36. Cooper-Sarkar, A. & Sarkar, S. Predictions for high energy neutrino cross-sections from the ZEUS global PDF fits. *J. High Energy Phys.* **0801**, 075 (2008).

37. Aartsen, M. G. et al. Searches for sterile neutrinos with the IceCube detector. *Phys. Rev. Lett.* **117**, 071801 (2016).

38. Foreman-Mackey, D., Hogg, D. W., Lang, D. & Goodman, J. emcee: the MCMC hammer. *Publ. Astron. Soc. Pac.* **125**, 306–312 (2013).

39. Aartsen, M. G. et al. Determining neutrino oscillation parameters from atmospheric muon neutrino disappearance with three years of IceCube DeepCore data. *Phys. Rev. D* **91**, 072004 (2015).

40. Harris, R. A. & Stodolsky, L. Two state systems in media and "Turing's paradox". *Phys. Lett. B* **116**, 464–468 (1982).

41. Abraham, J. et al. Observation of the suppression of the flux of cosmic rays above 4×10^{19}eV. *Phys. Rev. Lett.***101**, 061101 (2008).

42. Aab, A. et al. Evidence for a mixed mass composition at the 'ankle' in the cosmic-ray spectrum. *Phys. Lett. B***762**, 288–295 (2016).

43. Chalmers, M. Interview: Steven Weinberg. *CERN Courier* **57**, 31–35 (2017).

44. Aartsen, M. G. et al. Evidence for high-energy extraterrestrial neutrinos at the IceCube detector. *Science* **342**, 1242856 (2013).

45. Stecker, F. W., Scully, S. T., Liberati, S. & Mattingly, D. Searching for traces of Planck-scale physics with high energy neutrinos. *Phys. Rev. D* **91**, 045009 (2015).

46. Argüelles, C. A., Katori, T. & Salvado, J. New physics in astrophysical neutrino flavor. *Phys. Rev. Lett.* **115**, 161303 (2015).

47. Aartsen, M. G. et al. Measurement of South Pole ice transparency with the IceCube LED calibration system. *Nucl. Instrum. Meth. A* **711**, 73–89 (2013).

48. Aartsen, M. G. et al. Measurement of the atmospheric ν_e spectrum with IceCube. *Phys. Rev. D* **91**, 122004 (2015).

49. Adrian-Martinez, S. et al. Letter of intent for KM3NeT 2.0. *J. Phys. G* **43**, 084001 (2016).

50. Aartsen, M. G. et al. IceCube-Gen2: a vision for the future of neutrino astronomy in Antarctica. Preprint at https://arxiv.org/abs/1412.5106 (2014).

51. Altmann, M. et al. GNO solar neutrino observations: Results for GNO I. *Phys. Lett. B* **490**, 16–26 (2000).

52. Abdurashitov, J. N. et al. Solar neutrino flux measurements by the Soviet–American Gallium Experiment(SAGE) for half the 22 year solar cycle. *J. Exp. Theor. Phys.* **95**, 181 (2002).

53. Hosaka, J. et al. Solar neutrino measurements in super-Kamiokande-I. *Phys. Rev. D.* **73**, 112001 (2006).

54. Aharmim, B. et al. Electron energy spectra, fluxes, and day–night asymmetries of B-8 solar neutrinos from measurements with NaCl dissolved in the heavy-water detector at the Sudbury Neutrino Observatory. *Phys. Rev. C* **72**, 055502 (2005).

55. Arpesella, C. et al. Direct measurement of the Be-7 solar neutrino flux with 192 days of Borexino data. *Phys. Rev. Lett.* **101**, 091302 (2008).

56. Ashie, Y. et al. Evidence for an oscillatory signature in atmospheric neutrino oscillation. *Phys. Rev. Lett.* **93**, 101801 (2004).

57. Adamson, P. et al. Combined analysis of $\nu_\mu$disappearance and $\nu_\mu \rightarrow \nu_e$ appearance in MINOS using accelerator and atmospheric neutrinos. *Phys. Rev. Lett.***112**, 191801 (2014).

58. Aartsen, M. G. et al. Measurement of atmospheric neutrino oscillations at 6–56 GeV with IceCube DeepCore. *Phys. Rev. Lett.* **120**, 071801 (2018).

59. Abe, S. et al. Precision measurement of neutrino oscillation parameters with KamLAND. *Phys. Rev. Lett.***100**, 221803 (2008).

60. Abe, Y. et al. Indication of reactor disappearance in the Double Chooz experiment. *Phys. Rev. Lett.* **108**, 131801 (2012).

61. Ahn, J. K. et al. Observation of reactor electron antineutrino disappearance in the RENO experiment. *Phys. Rev. Lett.* **108**, 191802 (2012).

62. An, F. P. et al. Spectral measurement of electron antineutrino oscillation amplitude and frequency at Daya Bay. *Phys. Rev. Lett.* **112**, 061801 (2014).

63. Abe, K. et al. Combined analysis of neutrino and antineutrino oscillations at T2K. *Phys. Rev. Lett.* **118**, 151801 (2017).

64. Adamson, P. et al. Constraints on oscillation parameters from ν_e appearance and ν_μ disappearance in NOvA. *Phys. Rev. Lett.* **118**, 231801 (2017).

65. Coleman, S. R. & Glashow, S. L. High-energy tests of Lorentz invariance. *Phys. Rev. D* **59**, 116008 (1999).

66. Amelino-Camelia, G., Ellis, J. R., Mavromatos, N. E., Nanopoulos, D. V. & Sarkar, S. Tests of quantum gravity from observations of gamma-ray bursts. *Nature* **393**, 763–765 (1998).

67. Colladay, D. & Kostelecký, V. A. CPT violation and the standard model. *Phys. Rev. D.* **55**, 6760–6774 (1997).

68. Colladay, D. & Kostelecký, V. A. Lorentz violating extension of the standard model. *Phys. Rev. D.* **58**, 116002 (1998).

69. Kostelecký, V. A. Gravity, Lorentz violation, and the standard model. *Phys. Rev. D.* **69**, 105009 (2004).

70. Auerbach, L. B. et al. Tests of Lorentz violation in $\bar{\nu}_\mu \rightarrow \bar{\nu}_e \bar{\nu}_\mu \rightarrow \bar{\nu}_e$ oscillations. *Phys. Rev. D* **72**, 076004 (2005).

71.Aguilar-Arevalo, A. A. et al. Test of Lorentz and CPT violation with short baseline neutrino oscillation excesses. *Phys. Lett. B* **718**, 1303–1308 (2013).

72.Adamson, P. et al. Testing Lorentz invariance and CPT conservation with NuMI neutrinos in the MINOS near detector. *Phys. Rev. Lett.* **101**, 151601 (2008).

73.Adamson, P. et al. A search for Lorentz invariance and CPT violation with the MINOS far detector. *Phys. Rev. Lett.* **105**, 151601 (2010).

74.Adamson, P. et al. Search for Lorentz invariance and CPT violation with muon antineutrinos in the MINOS near detector. *Phys. Rev. D* **85**, 031101 (2012).

75.Rebel, B. & Mufson, S. The search for neutrino-antineutrino mixing resulting from Lorentz invariance violation using neutrino interactions in MINOS. *Astropart. Phys.* **48**, 78–81 (2013).

76.Abe, Y. et al. First test of Lorentz violation with a reactor-based antineutrino experiment. *Phys. Rev. D***86**, 112009 (2012).

77.Díaz, J. S., Katori, T., Spitz, J. & Conrad, J. M. Search for neutrino-antineutrino oscillations with a reactor experiment. *Phys. Lett. B* **727**, 412 (2013).

78.Diaz, J. S. & Schwetz, T. Limits on CPT violation from solar neutrinos. *Phys. Rev. D* **93**, 093004 (2016).

79.Abe, K. et al. Search for Lorentz and CPT violation using sidereal time dependence of neutrino flavor transitions over a short baseline. *Phys. Rev. D* **95**, 111101 (2017).

80.Feroz, F., Hobson, M. P. & Bridges, M. MultiNest: an efficient and robust Bayesian inference tool for cosmology and particle physics. *Mon. Not. R. Astron. Soc.* **398**, 1601–1614 (2009).

Acknowledgements

We acknowledge the support from the following agencies: USA—US National Science Foundation–Office of Polar Programs, US National Science Foundation–Physics Division, Wisconsin Alumni Research Foundation, Center for High Throughput Computing (CHTC) at the University of Wisconsin–Madison, Open Science Grid (OSG), Extreme Science and Engineering Discovery Environment (XSEDE), US Department of Energy–National Energy Research Scientific Computing Center, Particle astrophysics research computing centre at the University of Maryland, Institute for Cyber-Enabled Research at Michigan State University and Astroparticle physics computational facility at Marquette University; Belgium—Funds for Scientific Research (FRS-FNRS and FWO), FWO Odysseus and Big Science programmes, and Belgian Federal Science Policy Office (Belspo); Germany—Bundesministerium für Bildung und Forschung (BMBF), Deutsche Forschungsgemeinschaft (DFG), Helmholtz Alliance for Astroparticle Physics (HAP), Initiative and Networking Fund of the Helmholtz Association, Deutsches Elektronen Synchrotron (DESY), and High Performance Computing cluster of the RWTH Aachen; Sweden—Swedish Research Council, Swedish Polar Research Secretariat, Swedish National Infrastructure for Computing (SNIC), and Knut and Alice Wallenberg Foundation; Australia—Australian Research Council; Canada—Natural Sciences and Engineering Research Council of Canada, Calcul Québec, Compute Ontario, Canada Foundation for Innovation, WestGrid and Compute Canada; Denmark—Villum Fonden, Danish National Research Foundation (DNRF); New Zealand—Marsden Fund; Japan—Japan Society for Promotion of Science (JSPS) and Institute for Global Prominent Research (IGPR) of Chiba University; Korea—National Research Foundation of Korea (NRF); Switzerland—Swiss National Science Foundation (SNSF); UK—Science and Technology Facilities Council (STFC) and The Royal Society.

Author information

Affiliations

Department of Physics, University of Adelaide, Adelaide, Australia

- M. G. Aartsen
- G. C. Hill
- A. Kyriacou
- S. Robertson
- A. Wallace
- B. J. Whelan

DESY, Zeuthen, Germany

- M. Ackermann
- E. Bernardini
- S. Blot
- F. Bradascio
- H.-P. Bretz
- J. Brostean-Kaiser
- A. Franckowiak
- E. Jacobi
- T. Karg
- T. Kintscher
- S. Kunwar
- R. Nahnhauer
- K. Satalecka
- C. Spiering
- J. Stachurska
- A. Stasik
- N. L. Strotjohann
- A. Terliuk
- M. Usner
- J. van Santen
- M. Kowalski

Department of Physics and Astronomy, University of Canterbury, Christchurch, New Zealand

- J. Adams
- H. Bagherpour

Science Faculty, Université Libre de Bruxelles, Brussels, Belgium

- J. A. Aguilar
- I. Ansseau
- D. Heereman
- K. Meagher
- T. Meures
- A. O'Murchadha

- E. Pinat
- C. Raab

Niels Bohr Institute, University of Copenhagen, Copenhagen, Denmark

- M. Ahlers
- E. Bourbeau
- D. J. Koskinen
- M. J. Larson
- M. Medici
- M. Rameez
- T. Stuttard
- S. Sarkar

Oskar Klein Centre and Department of Physics, Stockholm University, Stockholm, Sweden

- M. Ahrens
- C. Bohm
- J. P. Dumm
- C. Finley
- S. Flis
- K. Hultqvist
- C. Walck
- M. Zoll

Département de physique nucléaire et corpusculaire, Université de Genève, Geneva, Switzerland

- I. Al Samarai
- S. Bron
- T. Carver
- A. Christov
- T. Montaruli

Erlangen Centre for Astroparticle Physics, Friedrich-Alexander-Universität Erlangen-Nürnberg, Erlangen, Germany

- D. Altmann
- G. Anton
- T. Glüsenkamp
- U. Katz
- T. Kittler
- M. Tselengidou

Department of Physics, Marquette University, Milwaukee, WI, USA

- K. Andeen
- M. Plum

Department of Physics, Pennsylvania State University, University Park, PA, USA

- T. Anderson
- J. J. DeLaunay
- M. Dunkman
- P. Eller
- F. Huang
- A. Keivani
- J. L. Lanfranchi
- D. V. Pankova
- G. Tešić
- C. F. Turley
- M. J. Weiss
- D. F. Cowen

Department of Physics, Massachusetts Institute of Technology, Cambridge, MA, USA

- C. Argüelles
- S. Axani
- G. H. Collin
- J. M. Conrad
- M. Moulai

III. Physikalisches Institut, RWTH Aachen University, Aachen, Germany

- J. Auffenberg
- M. Brenzke
- T. Glauch
- C. Haack
- P. Kalaczynski
- J. P. Koschinsky
- M. Leuermann
- L. Rädel
- R. Reimann
- M. Rongen
- T. Sälzer
- S. Schoenen
- L. Schumacher
- J. Stettner
- M. Vehring
- E. Vogel
- M. Wallraff
- A. Waza
- C. H. Wiebusch

Physics Department, South Dakota School of Mines and Technology, Rapid City, SD, USA

- X. Bai
- E. Dvorak

Department of Physics, University of Alberta, Edmonton, Alberta, Canada

- J. P. Barron
- W. Giang
- D. Grant
- C. Kopper
- R. W. Moore
- S. C. Nowicki
- S. E. Sanchez Herrera
- S. Sarkar
- F. D. Wandler
- C. Weaver
- T. R. Wood
- E. Woolsey
- J. P. Yanez

Department of Physics and Astronomy, University of California, Irvine, CA, USA

- S. W. Barwick
- G. Yodh

Institute of Physics, University of Mainz, Mainz, Germany

- V. Baum
- S. Böser
- V. di Lorenzo
- B. Eberhardt
- T. Ehrhardt
- L. Köpke
- G. Krückl
- G. Momenté
- P. Peiffer
- J. Sandroos
- A. Steuer
- K. Wiebe

Department of Physics, University of California, Berkeley, CA, USA

- R. Bay
- K. Filimonov
- P. B. Price
- K. Woschnagg
- G. Binder
- S. R. Klein
- S. Miarecki
- T. Palczewski
- J. Tatar

Department of Physics and Center for Cosmology and Astro-Particle Physics, Ohio State University, Columbus, OH, USA

- J. J. Beatty
- M. Stamatikos
- M. Sutherland

Department of Astronomy, Ohio State University, Columbus, OH, USA

- J. J. Beatty

Fakultät für Physik & Astronomie, Ruhr-Universität Bochum, Bochum, Germany

- J. Becker Tjus
- F. Bos
- B. Eichmann
- M. Kroll
- S. Schöneberg
- F. Tenholt

Department of Physics, University of Wuppertal, Wuppertal, Germany

- K.-H. Becker
- D. Bindig
- K. Helbing
- S. Hickford
- R. Hoffmann
- F. Lauber
- U. Naumann
- A. Obertacke Pollmann
- D. Soldin

Department of Physics and Astronomy, University of Rochester, Rochester, NY, USA

- S. BenZvi
- R. Cross

Department of Physics, University of Maryland, College Park, MD, USA

- D. Berley
- E. Blaufuss
- E. Cheung
- J. Felde
- E. Friedman
- R. Hellauer
- K. D. Hoffman
- R. Maunu
- A. Olivas
- T. Schmidt

- M. Song
- G. W. Sullivan

Department of Physics and Astronomy, University of Kansas, Lawrence, KS, USA

- D. Z. Besson

Lawrence Berkeley National Laboratory, Berkeley, CA, USA

- G. Binder
- S. R. Klein
- S. Miarecki
- T. Palczewski
- J. Tatar
- L. Gerhardt
- A. Goldschmidt
- D. R. Nygren
- G. T. Przybylski
- T. Stezelberger
- R. G. Stokstad

Department of Physics, TU Dortmund University, Dortmund, Germany

- M. Börner
- T. Fuchs
- M. Hünnefeld
- M. Meier
- T. Menne
- D. Pieloth
- W. Rhode
- T. Ruhe
- A. Sandrock
- P. Schlunder
- J. Soedingrekso
- J. Werthebach

Department of Physics, Sungkyunkwan University, Suwon, Korea

- D. Bose
- H. Dujmovic
- S. In
- M. Jeong
- W. Kang
- J. Kim
- C. Rott

Department of Physics and Astronomy, Uppsala University, Uppsala, Sweden

- O. Botner

- A. Burgman
- A. Hallgren
- C. Pérez de los Heros
- E. Unger

Department of Physics and Wisconsin IceCube Particle Astrophysics Center, University of Wisconsin, Madison, WI, USA

- J. Bourbeau
- J. Braun
- J. Casey
- D. Chirkin
- M. Day
- P. Desiati
- J. C. Díaz-Vélez
- S. Fahey
- K. Ghorbani
- Z. Griffith
- F. Halzen
- K. Hanson
- B. Hokanson-Fasig
- K. Jero
- A. Karle
- M. Kauer
- J. L. Kelley
- A. Kheirandish
- Q. R. Liu
- W. Luszczak
- S. Mancina
- F. McNally
- G. Merino
- A. Schneider
- M. N. Tobin
- D. Tosi
- B. Ty
- J. Vandenbroucke
- N. Wandkowsky
- C. Wendt
- S. Westerhoff
- L. Wille
- M. Wolf
- J. Wood
- D. L. Xu
- T. Yuan
- K. Hoshina

Dienst ELEM, Vrije Universiteit Brussel (VUB), Brussels, Belgium

- L. Brayeur
- M. Casier

- C. De Clercq
- K. D. de Vries
- G. de Wasseige
- J. Kunnen
- J. Lünemann
- G. Maggi
- S. Toscano
- N. van Eijndhoven

SNOLAB, Lively, ON, Canada

- K. Clark

Institut für Kernphysik, Westfälische Wilhelms-Universität Münster, Münster, Germany

- L. Classen
- A. Kappes

Physik-department, Technische Universität München, Garching, Germany

- S. Coenders
- M. Huber
- K. Krings
- I. C. Rea
- E. Resconi
- A. Turcati

Department of Astronomy and Astrophysics, Pennsylvania State University, University Park, PA, USA

- D. F. Cowen

Department of Physics and Astronomy, Michigan State University, East Lansing, MI, USA

- J. P. A. M. de André
- T. DeYoung
- J. Hignight
- K. B. M. Mahn
- J. Micallef
- G. Neer
- D. Rysewyk

Bartol Research Institute and Department of Physics and Astronomy, University of Delaware, Newark, DE, USA

- H. Dembinski
- P. A. Evenson
- T. K. Gaisser
- J. G. Gonzalez
- R. Koirala

- H. Pandya
- D. Seckel
- T. Stanev
- S. Tilav

Department of Physics and Astronomy, University of Gent, Gent, Belgium

- S. De Ridder
- M. Labare
- D. Ryckbosch
- W. Van Driessche
- S. Vanheule
- M. Vraeghe

Institut für Physik, Humboldt-Universität zu Berlin, Berlin, Germany

- M. de With
- D. Hebecker
- H. Kolanoski
- M. Kowalski

Department of Physics, Southern University, Baton Rouge, LA, USA

- A. R. Fazely
- S. Ter-Antonyan
- X. W. Xu

Department of Astronomy, University of Wisconsin, Madison, WI, USA

- J. Gallagher

Earthquake Research Institute, University of Tokyo, Bunkyo, Tokyo, Japan

- K. Hoshina

Department of Physics and Institute for Global Prominent Research, Chiba University, Chiba, Japan

- A. Ishihara
- M. Kim
- T. Kuwabara
- L. Lu
- K. Mase
- M. Relich
- A. Stößl
- S. Yoshida

CTSPS, Clark-Atlanta University, Atlanta, GA, USA

- G. S. Japaridze

Department of Physics, University of Texas at Arlington, Arlington, TX, USA

- B. J. P. Jones

School of Physics and Astronomy, Queen Mary University of London, London, UK

- T. Katori
- S. Mandalia

Department of Physics and Astronomy, Stony Brook University, Stony Brook, NY, USA

- J. Kiryluk
- M. Lesiak-Bzdak
- H. Niederhausen
- Y. Xu

Universitee de Mons, Mons, Belgium

- G. Kohnen

Department of Physics and Astronomy, University of Alabama, Tuscaloosa, AL, USA

- S. Kopper
- P. Nakarmi
- J. A. Pepper
- M. Santander
- P. A. Toale
- D. R. Williams

Department of Physics, Drexel University, Philadelphia, PA, USA

- N. Kurahashi
- B. Relethford
- M. Richman
- L. Wills

Department of Physics, University of Wisconsin, River Falls, WI, USA

- J. Madsen
- S. Seunarine
- G. M. Spiczak

Department of Physics, Yale University, New Haven, CT, USA

- R. Maruyama

Department of Physics and Astronomy, University of Alaska Anchorage, Anchorage, AK, USA

- K. Rawlins

Department of Physics, University of Oxford, Oxford, UK

- S. Sarkar

School of Physics and Center for Relativistic Astrophysics, Georgia Institute of Technology, Atlanta, GA, USA

- I. Taboada
- C. F. Tung

Consortia

The IceCube Collaboration

- M. G. Aartsen
- G. C. Hill
- A. Kyriacou
- S. Robertson
- A. Wallace
- B. J. Whelan
- M. Ackermann
- E. Bernardini
- S. Blot
- F. Bradascio
- H.-P. Bretz
- J. Brostean-Kaiser
- A. Franckowiak
- E. Jacobi
- T. Karg
- T. Kintscher
- S. Kunwar
- R. Nahnhauer
- K. Satalecka
- C. Spiering
- J. Stachurska
- A. Stasik
- N. L. Strotjohann
- A. Terliuk
- M. Usner
- J. van Santen
- J. Adams
- H. Bagherpour
- J. A. Aguilar
- I. Ansseau
- D. Heereman
- K. Meagher

- T. Meures
- A. O’Murchadha
- E. Pinat
- C. Raab
- M. Ahlers
- E. Bourbeau
- D. J. Koskinen
- M. J. Larson
- M. Medici
- M. Rameez
- T. Stuttard
- M. Ahrens
- C. Bohm
- J. P. Dumm
- C. Finley
- S. Flis
- K. Hultqvist
- C. Walck
- M. Zoll
- I. Al Samarai
- S. Bron
- T. Carver
- A. Christov
- T. Montaruli
- D. Altmann
- G. Anton
- T. Glüsenkamp
- U. Katz
- T. Kittler
- M. Tselengidou
- K. Andeen
- M. Plum
- T. Anderson
- J. J. DeLaunay
- M. Dunkman
- P. Eller
- F. Huang
- A. Keivani
- J. L. Lanfranchi
- D. V. Pankova
- G. Tešić
- C. F. Turley
- M. J. Weiss
- C. Argüelles
- S. Axani
- G. H. Collin
- J. M. Conrad
- M. Moulai
- J. Auffenberg
- M. Brenzke

- T. Glauch
- C. Haack
- P. Kalaczynski
- J. P. Koschinsky
- M. Leuermann
- L. Rädel
- R. Reimann
- M. Rongen
- T. Sälzer
- S. Schoenen
- L. Schumacher
- J. Stettner
- M. Vehring
- E. Vogel
- M. Wallraff
- A. Waza
- C. H. Wiebusch
- X. Bai
- E. Dvorak
- J. P. Barron
- W. Giang
- D. Grant
- C. Kopper
- R. W. Moore
- S. C. Nowicki
- S. E. Sanchez Herrera
- S. Sarkar
- F. D. Wandler
- C. Weaver
- T. R. Wood
- E. Woolsey
- J. P. Yanez
- S. W. Barwick
- G. Yodh
- V. Baum
- S. Böser
- V. di Lorenzo
- B. Eberhardt
- T. Ehrhardt
- L. Köpke
- G. Krückl
- G. Momenté
- P. Peiffer
- J. Sandroos
- A. Steuer
- K. Wiebe
- R. Bay
- K. Filimonov
- P. B. Price
- K. Woschnagg

- J. J. Beatty
- J. Becker Tjus
- F. Bos
- B. Eichmann
- M. Kroll
- S. Schöneberg
- F. Tenholt
- K.-H. Becker
- D. Bindig
- K. Helbing
- S. Hickford
- R. Hoffmann
- F. Lauber
- U. Naumann
- A. Obertacke Pollmann
- D. Soldin
- S. BenZvi
- R. Cross
- D. Berley
- E. Blaufuss
- E. Cheung
- J. Felde
- E. Friedman
- R. Hellauer
- K. D. Hoffman
- R. Maunu
- A. Olivas
- T. Schmidt
- M. Song
- G. W. Sullivan
- D. Z. Besson
- G. Binder
- S. R. Klein
- S. Miarecki
- T. Palczewski
- J. Tatar
- M. Börner
- T. Fuchs
- M. Hünnefeld
- M. Meier
- T. Menne
- D. Pieloth
- W. Rhode
- T. Ruhe
- A. Sandrock
- P. Schlunder
- J. Soedingrekso
- J. Werthebach
- D. Bose
- H. Dujmovic

- S. In
- M. Jeong
- W. Kang
- J. Kim
- C. Rott
- O. Botner
- A. Burgman
- A. Hallgren
- C. Pérez de los Heros
- E. Unger
- J. Bourbeau
- J. Braun
- J. Casey
- D. Chirkin
- M. Day
- P. Desiati
- J. C. Díaz-Vélez
- S. Fahey
- K. Ghorbani
- Z. Griffith
- F. Halzen
- K. Hanson
- B. Hokanson-Fasig
- K. Jero
- A. Karle
- M. Kauer
- J. L. Kelley
- A. Kheirandish
- Q. R. Liu
- W. Luszczak
- S. Mancina
- F. McNally
- G. Merino
- A. Schneider
- M. N. Tobin
- D. Tosi
- B. Ty
- J. Vandenbroucke
- N. Wandkowsky
- C. Wendt
- S. Westerhoff
- L. Wille
- M. Wolf
- J. Wood
- D. L. Xu
- T. Yuan
- L. Brayeur
- M. Casier
- C. De Clercq
- K. D. de Vries

- G. de Wasseige
- J. Kunnen
- J. Lünemann
- G. Maggi
- S. Toscano
- N. van Eijndhoven
- K. Clark
- L. Classen
- A. Kappes
- S. Coenders
- M. Huber
- K. Krings
- I. C. Rea
- E. Resconi
- A. Turcati
- D. F. Cowen
- J. P. A. M. de André
- T. DeYoung
- J. Hignight
- K. B. M. Mahn
- J. Micallef
- G. Neer
- D. Rysewyk
- H. Dembinski
- P. A. Evenson
- T. K. Gaisser
- J. G. Gonzalez
- R. Koirala
- H. Pandya
- D. Seckel
- T. Stanev
- S. Tilav
- S. De Ridder
- M. Labare
- D. Ryckbosch
- W. Van Driessche
- S. Vanheule
- M. Vraeghe
- M. de With
- D. Hebecker
- H. Kolanoski
- A. R. Fazely
- S. Ter-Antonyan
- X. W. Xu
- J. Gallagher
- L. Gerhardt
- A. Goldschmidt
- D. R. Nygren
- G. T. Przybylski
- T. Stezelberger

- R. G. Stokstad
- K. Hoshina
- A. Ishihara
- M. Kim
- T. Kuwabara
- L. Lu
- K. Mase
- M. Relich
- A. Stößl
- S. Yoshida
- G. S. Japaridze
- B. J. P. Jones
- T. Katori
- S. Mandalia
- J. Kiryluk
- M. Lesiak-Bzdak
- H. Niederhausen
- Y. Xu
- G. Kohnen
- S. Kopper
- P. Nakarmi
- J. A. Pepper
- M. Santander
- P. A. Toale
- D. R. Williams
- M. Kowalski
- N. Kurahashi
- B. Relethford
- M. Richman
- L. Wills
- J. Madsen
- S. Seunarine
- G. M. Spiczak
- R. Maruyama
- K. Rawlins
- S. Sarkar
- M. Stamatikos
- M. Sutherland
- I. Taboada
- C. F. Tung

Contributions

The IceCube Collaboration designed, constructed and now operates the IceCube Neutrino Observatory. Data processing and calibration, Monte Carlo simulations of the detector and of theoretical models, and data analyses were performed by a large number of collaboration members, who also discussed and approved the scientific results presented here. The main authors of this manuscript were C. Argüelles, A. Kheirandish, G. Collin, S. Mandalia, J. Conrad and T. Katori. It was reviewed by the entire collaboration before publication, and all authors approved the final version of the manuscript.

Competing interests

The authors declare no competing interests.

Corresponding authors

Correspondence to C. Argüelles or G. H. Collin or J. M. Conrad or A. Kheirandish or T. Katori or S. Mandalia.